Quantum Battery with Non-Hermitian Charging

Tanoy Kanti Konar, Leela Ganesh Chandra Lakkaraju, Aditi Sen (De)
Harish-Chandra Research Institute, A CI of Homi Bhabha National Institute, Chhatnag Road, Jhunsi, Prayagraj - 211019, India

We propose a design of a quantum battery exploiting the non-Hermitian Hamiltonian as a charger. In particular, starting with the ground or the thermal state of the interacting (non-interacting) Hamiltonian as the battery, the charging of the battery is performed via $\mathcal{PT}$- ($\mathcal{RT}$)-symmetric Hamiltonian to store or extract energy. We report that such a quenching with a non-Hermitian Hamiltonian leads to an enhanced power output compared to a battery with a Hermitian charger. We identify the region in the parameter space which provides the gain in performance. We also demonstrate that the improvements persist with the increase of system size both in the battery having $\mathcal{PT}$- and $\mathcal{RT}$-symmetric charger. In the $\mathcal{PT}$-symmetric case, although the anisotropy of the XY model does not help in the performance, we show that the XXZ model as a battery with a non-Hermitian charger performs better than that of the XX model having certain interaction strengths. We also exhibit that the advantage of non-Hermiticity remains valid even at finite temperatures in the initial states.

I. INTRODUCTION

Miniaturization of technology with the usage of quantum mechanical principles has become an intensive field of research in recent times. Notable achievements exhibiting quantum advantage over their classical analogs, thereby revolutionizing the arena of modern technologies include quantum key distribution [1], quantum communication, [2, 3], quantum computers [4], and devices for metrology [5] like quantum sensors [6] to name a few. In this respect, designing quantum thermal machines like quantum refrigerator [7, 8], quantum battery [9, 10] and thermal transistor [11] have two-fold motivations – in one hand, it is important to understand the concepts of heat, work, and temperature in the microscopic limit, thereby developing the laws of quantum thermodynamics [12–14] and on the other hand, how to achieve the optimal performance from the machines even when there is a competition between thermal and quantum fluctuations. It is also an interdisciplinary field lying at the crossroads of quantum optics, non-equilibrium statistical mechanics, and quantum information theory. Moreover, with the increase of control on quantum systems, several experiments have been performed to verify quantum thermodynamical laws like Jarzynski equality [15–17] and thermal machines like quantum batteries [18, 19], quantum refrigerators [20] in several physical substrates like trapped ions, nuclear magnetic resonances, cold atoms, etc.

The original proposal for the quantum battery (QB) considers the initial battery-state as the ground state of a non-interacting Hamiltonian which can then be charged by global unitary operations [9, 10, 18, 21, 22]. The main goal of such construction is to show that the work output or power stored (extracted) in (from) the battery gets enhanced in presence of quantum mechanical systems or quantum operations. Instead of a non-interacting Hamiltonian, the ground or the thermal state of an interacting Hamiltonian can also be used as the battery [23, 24] while the local magnetic field in a suitable direction is applied at each site to maximize the energy storage of the battery. Such a design turns out to be appropriate even in presence of decoherence and disorder [24–26] as well as in higher dimension [27].

The evolution of a quantum system is described by a Hamiltonian which is typically a Hermitian operator. It was shown that relaxing Hermiticity condition, if one considers non-Hermitian systems with parity-time ($\mathcal{PT}$) symmetry [28, 29] (with $\mathcal{P}$ being the reflection operator in space and $\mathcal{T}$ being the time-reversal operator) or rotation-time ($\mathcal{RT}$) symmetry (with $\mathcal{R}$ being the rotation operator along a fixed axis) [30], the energy eigenvalues can be real depending on the system parameters, thereby maintaining all the properties of standard quantum mechanics and describing natural processes. However, such a system undergoes a transition from broken to an unbroken phase where the energy spectrum becomes real from imaginary values, known as exceptional points [28, 29]. Several counter-intuitive results are also reported in this framework – when a local $\mathcal{PT}$-symmetric Hamiltonian acts on a part of an entangled state, it was shown that there is a violation of no-signalling principle [31] which was later settled by Naimark's dilation [32]. On the other hand, interesting phases in the ground state of the $\mathcal{RT}$-symmetric Hamiltonian are also reported [30, 33, 34] in which the broken-unbroken transition is found to be connected with the factorization surface of the corresponding Hermitian models [35]. Over the times, it has been realized that such systems can have great influences in different branches of physics ranging from optics [36, 37] to electronics [38], Bose-Einstein condensates [39] and many-body physics [30, 33, 34, 40–43]. In this respect, it has also been realized that the performance of quantum sensors can be improved with non-Hermiticity [44–49].

Motivated by the advantages provided by non-Hermitian systems, we utilize non-Hermiticity to propose a set-up of a quantum battery. In particular, when the initial state of the battery is the ground states of the interacting and non-interacting Hamiltonian, we use $\mathcal{PT}$- as well as $\mathcal{RT}$-symmetric Hamiltonian to charge the battery. In both cases, we show that the power of the battery gets enhanced with the help of non-Hermitian charging Hamiltonian compared to their Hermitian counterparts. In particular, we identify a parameter region where such a beneficial role can be found. We demonstrate that the maximum power decreases with the anisotropy parameter of the XY model as a battery in the $\mathcal{PT}$-symmetric case and as a charger in the $\mathcal{RT}$-symmetric scenarios although, for a fixed anisotropy, non-Hermiticity still provides a benefit over the Hermitian set-up. We also observe that the energy that can be extracted, measured via ergotropy [9], coincides with the work output in the evolution and hence the power computed here quantifies both the storage as well as extractable power of the QB.

Moreover, the trends of the maximum power saturates to a finite values for a moderate system size both for batteries with the $\mathcal{PT}$- and $\mathcal{RT}$-symmetric chargers. When the initial state is the thermal state of the system, the maximum power decreases with the increase of temperature although some distinct behavior due to non-Hermitian evolution is observed in the limit of infinite temperature.

The paper is organized in the following manner. In Sec. II, we set the stage by introducing the quantities which quantify the performance of the battery. The design of the battery and its performance when it is charged with the $\mathcal{PT}$-symmetric Hamiltonian is presented in Sec. III. When the charger has $\mathcal{RT}$ symmetry, the results obtained are discussed in Sec. IV. The concluding remarks is given in the last section, Sec. V.

II. MODELLING QUANTUM BATTERY AND ITS FIGURES OF MERITS

A design of a quantum battery has two components – 1. the battery Hamiltonian, and 2. a charger. In this work, we choose both ground and the thermal states of interacting as well as non-interacting Hamiltonians, H_B as the initial state of the battery. The details of these Hamiltonians will be discussed in succeeding sections.

Charging. In general, a charging Hamiltonian is used to excite the particles to a higher energy state so that the high amount of energy gets stored in the QB which can be extracted from the battery in a suitable time by a unitary operation. In this work, instead of Hermitian Hamiltonian, two non-Hermitian Hamiltonians having parity(rotation)-time symmetry, $H_{charging}^{\mathcal{PT}(\mathcal{RT})}$ are used independently as chargers of the battery. Specifically, we use the well known quantum $\mathcal{PT}$-symmetric Hamiltonian [31] and $\mathcal{RT}$-symmetric XY-model [30] for the purpose of charging (for details, see Secs. III and IV).

The performance of a quantum Battery is decided by the amount of generated power. In order to describe that, we need the thermodynamic definition of work.

Work and power. The work output at a given time instance can be measured as [9, 10] $W(t) = \text{tr}[H_B(\rho(t) - \rho(0))]$, where $\rho(0)$ is the initial state of the battery Hamiltonian, which are taken to be the ground or the thermal states of H_B while $\rho(t)$ is obtained after evolving the system with non-Hermitian Hamiltonian, given by $\rho(t) = (1/\mathcal{N}) \exp\left(-iH_{charging}^{\mathcal{PT}(\mathcal{RT})}t\right)\rho(0)\exp\left(iH_{charging}^{\mathcal{PT}(\mathcal{RT})}t\right)$ with $\mathcal{N} = \text{tr}[\exp\left(-iH_{charging}^{\mathcal{PT}(\mathcal{RT})}t\right)\rho(0)\exp\left(iH_{charging}^{\mathcal{PT}(\mathcal{RT})}t\right)]$. Notice that unlike unitary dynamics governed by a Hermitian Hamiltonian, we need to normalize the evolved state at each time interval in the non-Hermitian domain. The maximal power can be computed by performing maximization over time as

$$P_{max} = \max_t \frac{W(t)}{t} = \max_t P(t), \quad (1)$$

where $P(t)$ denotes the instantaneous power at some time, $t > 0$. In our case, even in presence of non-Hermiticity, $P(t)$ is always found to be real.

In general, when the value of a parameter, e.g., the applied magnetic field, increases, the amount of power generated trivially increases. In order to maintain a fair comparison between different situations, we normalize the battery Hamiltonian as

$$\frac{1}{E_{\max} - E_{\min}}[2H_B - (E_{\max} + E_{\min})\mathcal{I}] \rightarrow H_B, \quad (2)$$

where the minimum and maximum eigenenergies are denoted by $E_{\min}$ and $E_{\max}$ respectively. Thus, the spectrum is bounded between $[-1, 1]$ which ensures that the advantage is not the artifact of the parameters.

As mentioned, the energy stored in the battery can be represented as $W(t)$ although the entire energy may not be extractable. In other words, the energy that can be extracted from the battery may not always coincide with the work output in several scenarios including when the battery is in contact with the environment [25, 26]. The extractable energy, known as ergotropy, from the battery at some time instance t can be quantified as [9, 25, 50]

$$\mathcal{E} = E_B(t) - \min_{U'_{charging}} \text{tr}(H_B\rho(t)), \quad (3)$$

where $E_B(t) = \text{tr}(H_B\rho(t))$ is the energy at some time instant and $U'_{charging} = \exp\left(-iH_{charging}^{\mathcal{PT}(\mathcal{RT})}t\right)$ is the evolution operator due to the charging Hamiltonian which is taken either to be $\mathcal{PT}$- or $\mathcal{RT}$-symmetric Hamiltonian. In our case, the stored energy $W(t)$ and ergotropy $\mathcal{E}$ coincides (see the behavior of $\mathcal{E}$ in Fig. 1).

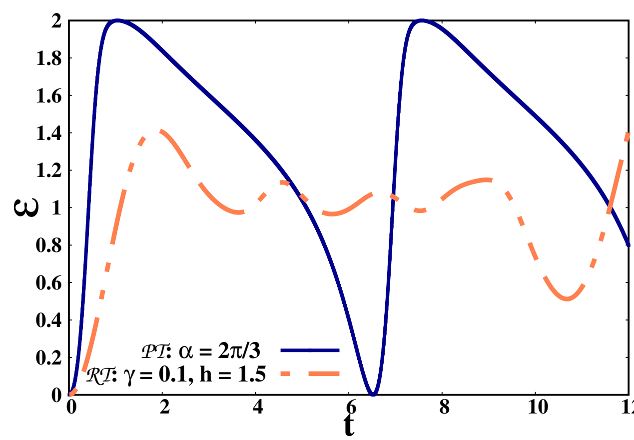

FIG. 1. (Color online.) **Ergotropy with $\mathcal{PT}$- and $\mathcal{RT}$-symmetric chargers.** Variation of ergotropy, $\mathcal{E}$ (vertical axis) with time t (horizontal axis). In the $\mathcal{PT}$-symmetric charger with $\alpha = 2pi/3$ (solid line), the initial battery Hamiltonian is taken to be the ground state of the XX model while in the $\mathcal{RT}$-symmetric charger with $\gamma = 0.1, h = 1.5$ (dashed-dot line), it is the ground state of the non-interacting Hamiltonian. Here $N = 6$. It can be shown that the work output, $W(t)$ of the battery coincides with the ergotropy, thereby ensuring the equality between the stored and extractable energy with time. Both the axes are dimensionless.

III. ENHANCEMENT OF POWER WITH $\mathcal{PT}$ SYMMETRIC CHARGER

Let us describe briefly the set-up of a quantum battery and the charger in the non-Hermitian framework. The ground or the thermal state of the XYZ Hamiltonian in presence of transverse magnetic field, given by

$$H_B = \frac{J}{4}\sum_{r=1}^{N}\left[(1+\gamma)\sigma_r^x\sigma_{r+1}^x + (1-\gamma)\sigma_r^y\sigma_{r+1}^y\right] + \frac{\Delta}{4}\sum_{r=1}^{N}\sigma_r^z\sigma_{r+1}^z + \frac{h}{2}\sum_{r=1}^{N}\sigma_r^z, \quad (4)$$

act as the battery. Here σ^i-matrices represent the Pauli matrices, γ corresponds to the anisotropy in the xy-plane, J and Δ are the coupling constants in the xy-plane and z direction respectively and h is the strength of the magnetic field in the transverse direction. Notice that with available technologies, the above Hamiltonian can be controlled and manipulated using physical systems like cold atoms, trapped ions, nuclear magnetic resonances [51–54].

$\mathcal{PT}$-symmetric Hamiltonian as a Charger. The quantum battery is charged by using a local $\mathcal{PT}$-symmetric Hamiltonian which can be simulated in the laboratory [32, 55] as a dilation of higher dimensional Hilbert space [56–58]. It is expressed as

$$H^{\mathcal{PT}}_{charging} = \sum_{r=1}^{N}\left[\sigma_r^x + i\sin\alpha\sigma_r^z\right], \quad (5)$$

where the Hamiltonian possess parity symmetry, i.e., $\mathcal{P}$ acts on the Hamiltonian, $\mathcal{P}H^{\mathcal{PT}}_{charging}\mathcal{P} = H^{*\mathcal{PT}}_{charging}$ while $\mathcal{T}$ is a simple complex conjugation in finite dimension, $\mathcal{T}i\mathcal{T} = -i$. Here α is the $\mathcal{PT}$-symmetry (non-Hermiticity) parameter of $H^{\mathcal{PT}}_{charging}$ and $\alpha = \pi/2$ represents the exceptional point (EP) where eigenvectors and eigenvalues of the local charging Hamiltonian coalesces. At $\alpha = 0$, the Hamiltonian reduces to the Hermitian one. Instead of taking $\alpha = 0$ which changes the magnetic field only in the z direction, we can consider Hermitian charger as

$$H^{herm}_{charging} = \sum_{r=1}^{N}\left[\sigma_r^x + \sin\alpha\sigma_r^z\right], \quad (6)$$

and the corresponding instantaneous power of the QB is denoted by P^{herm} while $P^{\mathcal{PT}}$ represents the same with $\mathcal{PT}$-symmetric charger. Notice that in this way, both of them are functions of α.

Before considering the general battery Hamiltonian, let us first illustrate the effects of non-Hermiticity on the performance of the QB when the initial state is the ground state of the XX model, i.e., H_B with $\gamma = 0$ and $\Delta = 0$. Before proceeding to compute the maximal power produced from the battery, let us first manifest the behavior of ergotropy with time and compare it with the work output for fixed values of α. Unlike noisy scenarios, we find that the ergotropy, shown in Fig. 1 and the work output match for different non-zero values of α.

In this scenario, when there are two sites, we obtain the following proposition on enhancement.

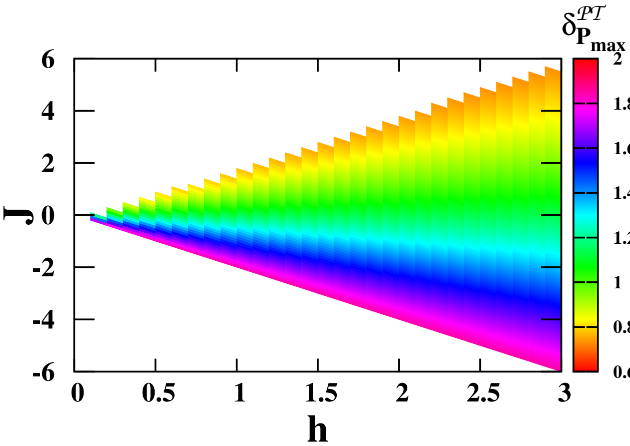

FIG. 2. **Non-Hermitian vs. Hermitian.** Map plot of $\delta^{\mathcal{PT}}_{P_{\max}}$, the difference in maximum power obtained from the $\mathcal{PT}$-symmetric charging given in Eq. (5) and the corresponding Hermitian charging Hamiltonian, given in Eq. (6), with respect to J (vertical axis) and h (horizontal axis) of the battery Hamiltonian, H_B with $\gamma = \Delta = 0$, the XX model. The initial state is prepared as the ground state in the XX model of the QB when $J \in [-2h, 2h - 0.1]$. Here $N = 2$.

Proposition 1. *The maximum power output of the battery made out of two lattice sites in the presence of $\mathcal{PT}$-symmetry charger, $P^{\mathcal{PT}}$ is higher than that of a QB which is charged by the Hermitian Hamiltonian, when the initial state is the ground state of the XX model with $J \in [-2h, 2h - 0.1]$.*

Proof. The ground state, $|\psi(0)\rangle$ as the initial state of the XX model takes the form $|0001\rangle$ in the computational basis when $J \in \{-2h, 2h - 0.1\}$. After evolution with local $\mathcal{PT}$-symmetric charging Hamiltonian, the evolved state at time t, $|\psi(t)\rangle$ can be expressed (see Appendix) as a function of non-Hermitian parameter, α, and system parameters, J, h and time t. We can then straightforwardly compute the maximal power both for Hermitian and non-Hermitian cases (see Appendix for the expressions). To prove the enhancement due to non-Hermitian charger, we consider the quantity, called as the difference in maximum power between non-Hermitian and Hermitian domains, given by

$$\delta^{\mathcal{PT}}_{P_{\max}} = \max_t(P^{\mathcal{PT}}(t)) - \max_t(P^{herm}(t)), \quad (7)$$

which is also a function of α. As depicted in Fig. 2 for an exemplary value of $\alpha = \pi/3$, $\delta^{\mathcal{PT}}_{P_{\max}} > 0\ \forall\alpha$ with the battery Hamiltonian having $J \in \{-2h, 2h - 0.1\}$. ■

Let us now illustrate that the advantage persists even with the increase of system sizes, in presence of anisotropy in the battery Hamiltonian and exchange interaction in the z direction, i.e., with the XXZ model. The Proposition 1 shows that for a given α, $\delta_{P_{\max}}$ is nonvanishing.

Effects of non-Hermiticity and interactions on QB. We first examine the pattern of maximal extractable power $P_{\max}$

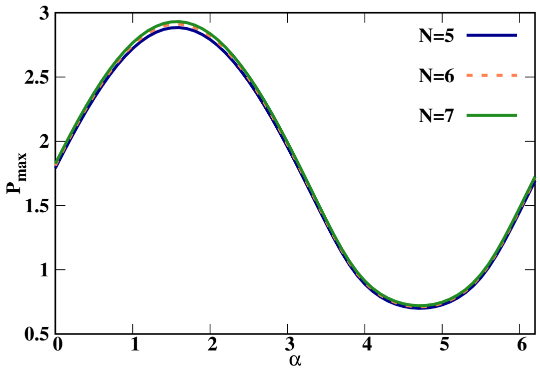

FIG. 3. (Color online) **Role of non-Hermiticity.** Maximum power output, $P_{\max}$ vs. non-Hermiticity parameter α in the charger. The effects of increase in system size is also depicted by taking different N values. The initial state of the QB is taken as in Fig. 2. Here $N = 6$, $J/|h| = 1$ and $\Delta = 0$ in the battery Hamiltonian, H_B in Eq. (4). All the axes are dimensionless.

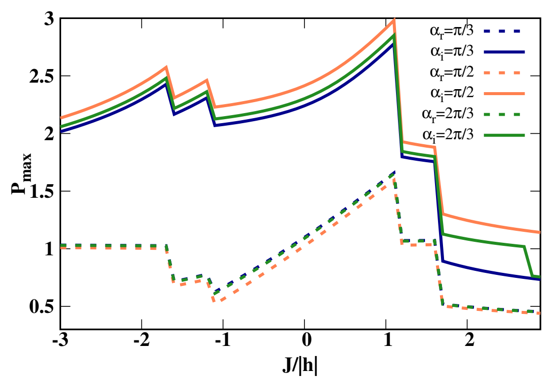

FIG. 4. (Color online) **Interaction dependence.** $P_{\max}$ (ordinate) against $J/|h|$ (abscissa) for different non-Hermiticity parameters, α. The XX model acts as the QB and the $\mathcal{PT}$-symmetric local charger in Eq. (5) is applied at each site of the battery. Solid lines represents Hermitian models, generating low power output while the dashed lines are for the non-Hermitian charger. Here $N = 6$. All the axes are dimensionless.

from the QB with the variation of α and the interaction strength in the xy-plane. A few observations immediately emerge from Figs. 3 and 4.

- Since the charging Hamiltonian involves $\sin\alpha$, the maximal power also shows the periodic nature with α as depicted in Fig. 3.
- Let us compare the power generated by the charging Hamiltonian possessing $\mathcal{PT}$-symmetry in Eq. (5) with $\alpha \neq 0$ and by the Hermitian charger, given in Eq. (6). We find that

$$P_{\max}^{herm} < P_{\max}^{\mathcal{PT}} \text{ for } (0 < \alpha < \pi). \quad (8)$$

  Note that in the region, the charging $\mathcal{PT}$-symmetric Hamiltonian has real energy spectrum [31].

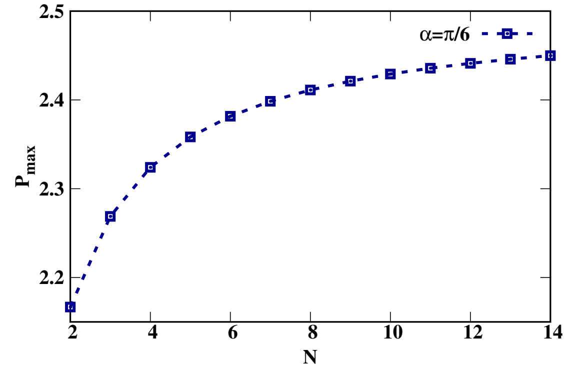

FIG. 5. (Color online) **Scaling.** $P_{\max}$ (ordinate) as a function of N (abscissa). All other specifications are same as in Fig. 3. Fitting the data shows that $P_{\max} \propto \sqrt{N}$. Both the axes are dimensionless.

- $P_{\max}$ reaches its maximum value with the charging Hamiltonian having $\alpha = \pi/2$ which is the exceptional point.
- The performance of the battery remains almost invariant with the increase of system size, N of the QB Hamiltonian. However, the scaling analysis of QB requires much more careful investigation which we will do next.
- It was shown that the QB can show quantum advantage (i.e., a QB is said to give quantum advantage when $P_{\max}$ obtained with the battery Hamiltonian having non vanishing interaction strength $J/|h| \neq 0$ is higher than that of the battery having vanishing interaction strength, i.e., $J/|h| = 0$ when the initial state of the battery is the ground state of the XX model [24]. We observe in Fig. 4 that non-Hermitian charging Hamiltonian can also provide quantum gain for different values of α. Moreover, unlike Hermitian situation, the quantum advantage in the non-Hermitian framework is observed both in the positive and negative regions of $J/|h|$ although the sharp continuous increase in the positive domain is not visible in the negative domain. This is possibly due to the fact that the charging battery Hamiltonian involves magnetic field both in the x and z directions while the initial state of the QB with low $J/|h|$ is prepared in the paramagnetic phase and hence after charging starts, there is competition between spins to keep in the z and x direction, thereby producing more power in this system.

Scaling analysis of QB. We now explore the quantum advantage in our model with the increase of sites in the lattice. For a fixed $\alpha > 0$, we find that $P_{\max}$ increases monotonically with N as depicted in Fig. 5. More careful analysis reveals that P_{max} scales not linearly with the system size. Specifically, we find

$$P_{\max} \propto \sqrt{N},$$

when the initial state of the QB is the ground state of the XX model with $J/|h| \in [-2h, 2h - 0.1]$.

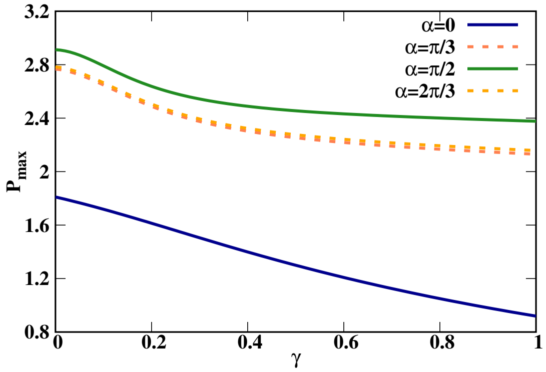

FIG. 6. (Color online) **Dependence on anisotropy.** $P_{\max}$ (vertical axis) with γ (horizontal axis) of the QB Hamiltonian for different values of α. $\alpha = 0$ represents the battery with a Hermitian charger. Other specifications are same as in Fig. 3. All the axes are dimensionless.

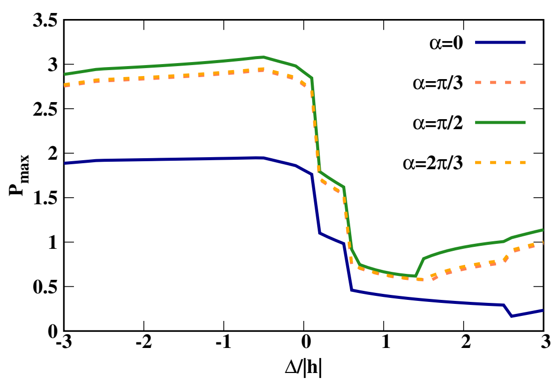

FIG. 7. (Color online) **Importance of the XXZ model as battery.** Trends of maximum power output, $P_{\max}$ with respect to the variation of interaction strength in the z direction, $\Delta/|h|$ for different values of α. Clearly, we observe that the XXZ model as a battery has some beneficial role over the XX model with $J/|h| = 1$. All other specifications are same as in Fig. 3. Both the axes are dimensionless.

Role of anisotropy and coupling in the z-direction. Upto now, the entire analysis is carried out when the initial battery Hamiltonian is the XX model. As shown in the Hermitian case [24, 27], the presence of anisotropy in the QB Hamiltonian typically suppresses the performance, i.e., $P_{\max}$ decreases with γ for a fixed α and $J/|h|$ which are chosen in the region where quantum advantage is seen (see Fig. 6). However, for nonvanishing α, we find that the rate of decrease in $P_{\max}$ after a certain anisotropy parameter diminishes with γ, i.e., after a sharp decrease with γ, $P_{\max}$ almost saturates for $\gamma > 0.5$ which was absent in the Hermitian counterpart as shown with $\alpha = 0$.

The introduction of interaction in the z direction also leads to a non trivial effect on QB's power extraction – for a fixed $J/|h|$, we find that with the decrease of $\Delta/|h|(< 0)$, $P_{\max}$ increases for different values of α and the maximum $P_{\max}$ is again obtained with the symmetry breaking transition point,

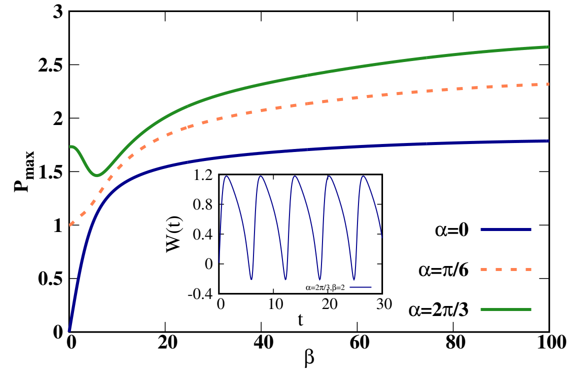

FIG. 8. (Color online) **Temperature-dependence of the initial state.** $P_{\max}$ (ordinate) vs. $\beta = 1/K_B T$ (abscissa) for different value of α. The initial state of the QB is prepared as the canonical equilibrium state of the XX model while the charger is the $\mathcal{PT}$-symmetric one with $\alpha \neq 0$. Notice that the decreasing behavior of the power with the increase of temperature is same as typically observed in the Hermitian domain. However, close to high temperature, in the framework of non-Hermitian systems, we find some different behavior than the one in Hermitian paradigm. (Inset) $W(t)$ with t for a fixed $\beta = 2.0$. It shows that $W(t)$ goes negative which is responsible for a nonmonotonic behavior of $P_{\max}$ at high temperature. All the axes are dimensionless.

i.e., $\alpha = \pi/2$ (as shown in Fig. 7).

A. Thermal state as initial state

It is not possible to achieve exact ground state of any Hamiltonian in laboratories. In particular, noise due to thermal fluctuation is unavoidable. To incorporate this imperfect situation, let us take the thermal state of the form, $\frac{\exp(-\beta' H_B)}{\text{tr}\{\exp(-\beta' H_B)\}}$ where $\beta' = 1/K_B T$ is inverse temperature (K_B being the Boltzmann constant and T is the temperature and we take $\beta = \beta'/|h|$) as the initial state of the QB. First of all, as one expects, we obtain the maximum power output from the battery even in the non-Hermitian framework, when the temperature of the thermal state is moderately low and $P_{\max}$ monotonically decreases with the increase of temperature (the decrease of β).

At high temperature, the certain abnormality arises in the non-Hermitian regime. In this respect, notice that with $\beta \to 0$, i.e., in presence of infinite temperature, the thermal state of a Hermitian Hamiltonian, H_B, reduces to the maximally mixed state. When the charging Hamiltonian is Hermitian and when the initial state is a thermal state with infinite temperature, the state does not evolve and so trivially the power of the QB vanishes. However, with the charging being the $\mathcal{PT}$-symmetric Hamiltonian, the process is no more unitary and it is debatable whether we can extract power even at high temperature as seen from Fig. 8.

IV. CHARGING BATTERY WITH $\mathcal{RT}$ SYMMETRIC HAMILTONIAN

Let us reverse the design of the QB and check whether the benefit due to non-Hermiticity still persists or not. Instead of an interacting Hamiltonian as the QB, let us take the initial state as the ground state of the non-interacting Hamiltonian, given by

$$H_B^{n-int} = \sum_{r=1}^{N} \sigma_r^x. \tag{9}$$

After normalizing the Hamiltonian, the eigenvector corresponding to the eigenvalue -1 is the initial state of the QB. A charging Hamiltonian in this case is taken to be the global non-Hermitian Hamiltonian, an XY model with imaginary anisotropy parameter, having $\mathcal{RT}$-symmetry, represented as

$$H_{charging}^{\mathcal{RT}} = \frac{J}{4}\sum_{r=1}^{N}\left[(1+i\gamma)\sigma_r^x\sigma_{r+1}^x + (1-i\gamma)\sigma_r^y\sigma_{r+1}^y\right] + \frac{h'}{2}\sum_{r=1}^{N}\sigma_r^z, \tag{10}$$

where the operator $\mathcal{R}$ rotates the spin by $\frac{\pi}{2}$, i.e., $\mathcal{R} \equiv e^{\left[-i(\pi/4)\sum_{j=1}^{N}\sigma_j^z\right]}$ and $\mathcal{T}$ is again the complex conjugation. Note that the charging Hamiltonian does not individually commute with either the operators, $[H_{charging}^{\mathcal{RT}}, \mathcal{R}] \neq 0$ or $[H_{charging}^{\mathcal{RT}}, \mathcal{T}] \neq 0$ although $[H_{charging}^{\mathcal{RT}}, \mathcal{RT}] = 0$, thereby making it a pseudo-Hermitian Hamiltonian. It has been shown that in the symmetry unbroken phase, the Hamiltonian has real eigenvalues while it contains complex conjugated imaginary eigenvalues in the broken phase [30] and the transition occurs when $h \equiv h'/|J| = \sqrt{1+\gamma^2}$.

In this scenario, when the initial battery Hamiltonian is non-interacting, the global operations are shown to be necessary to obtain quantum gain (quadratic scaling of power) which cannot be generated by the classical model [59]. We will first demonstrate that non-Hermitian charging Hamiltonian can produce more power than its Hermitian counterparts of a QB having two lattice sites.

Proposition 2. *The maximum power generated of a two-site quantum battery due to the $\mathcal{RT}$-symmetric XY charger with transverse magnetic field is greater than that of the Hermitian XY model provided the strength of the applied magnetic field is small and is strictly less than unity.*

Proof. To prove it, we compare the cases when the charging is Hermitian, i.e., $\gamma = -i\gamma'$ and when it is non-Hermitian, $\gamma = \gamma'$. We take the ground state of the normalized Hamiltonian, H_B^{n-int}, $|\psi(0)\rangle = \frac{1}{2}\begin{pmatrix}1\\-1\\-1\\1\end{pmatrix}$, with eigenvalue $=-1$ as the initial state of the QB. After applying the evolution due to the charging, the evolved state is, $|\psi(t)\rangle = \frac{e^{-iH_{charging}^{\mathcal{RT}}t}|\psi(0)\rangle}{\text{tr}[e^{-iH_{charging}^{\mathcal{RT}}t}|\psi(0)\rangle]} = |\psi(t)\rangle = \frac{1}{\sqrt{\mathcal{N}}}\begin{pmatrix}A\\B\\B\\C\end{pmatrix}$, where the expressions for A, B, C and $\mathcal{N}$ are given in Appendix. It is possible to compute $P^{\mathcal{RT}}(t)$ and the corresponding $P^{herm}(t)$ (see Appendix) and hence again we compute the difference

$$\delta_{P_{\max}}^{\mathcal{RT}} = \max_t(P^{\mathcal{RT}}(t)) - \max_t(P^{herm}(t)) \tag{11}$$

for $\gamma' \in \{0,1\}$ and $h \in \{0,2\}$. As shown in Fig. 9, there exists a region of h, i.e., when $h < 0.8$, $\delta_{P_{\max}}^{\mathcal{RT}} > 0$. It implies that the non-Hermitian charger clearly gives some benefit over the Hermitian ones. ■

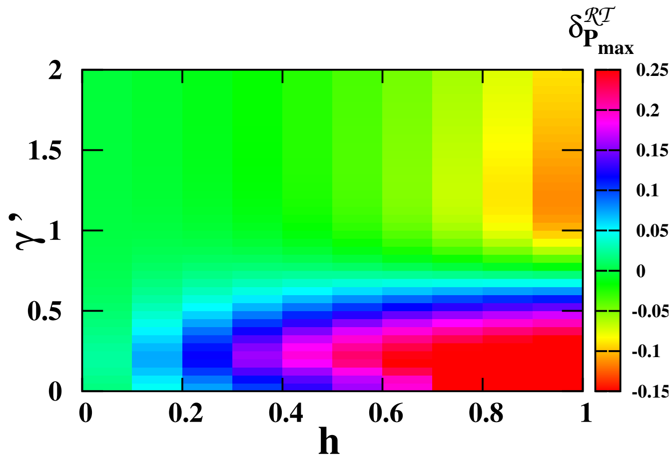

FIG. 9. **Non-Hermitian effects on QB.** Map plot of $\delta_{P_{\max}}^{\mathcal{RT}}$ with the variation of parameters in charging Hamiltonian, γ' (vertical axis) and h. The initial state is the ground state of the non-interacting battery Hamiltonian, H_B^{n-int} given in Eq. (**??**). Note that in Fig. 2, the difference was plotted with respect to battery Hamiltonian. However, both the plots manifest some advantage in presence of non-Hermitian charger over Hermitian one. Here $N = 2$.

Remark. The upper bound on h shown in Proposition 2 which is not unity is possibly due to the finite size effect. We will show in the scaling analysis, that with a moderate system size, the battery with a non-Hermitian charger provides a higher maximal power than that of the Hermitian ones when $h < 1.0$ irrespective of nonvanishing γ parameter which controls its non-Hermiticity.

Effect of $\mathcal{RT}$-symmetric charger on power. We compare the maximum power generated via non-Hermitian model corresponding to applied magnetic field, denoted with h_i and $P_{\max}$ produced by the Hermitian model having applied field, h_r with the variation of γ' in Fig. 10. It is evident that the difference between generated power by non-Hermitian and Hermitian charger, $\delta_{P_{\max}}^{\mathcal{RT}}$ is maximum when h is small, it decreases with the increase of h and finally becomes negative for high value of h, i.e., when $h > 1$. More precisely, the observations can be listed as follows.

1. When the $h_{i(r)} \sim 0.5 < 1.0$, the non-Hermitian charging admits higher P_{max} compared to the Hermitain

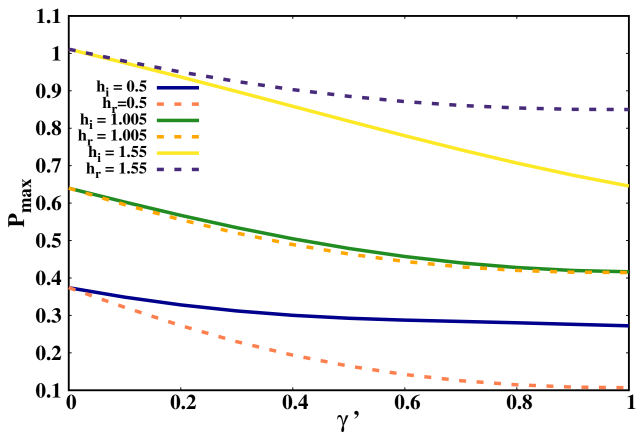

FIG. 10. **Comparison between Hermitian and non-Hermitian chargers.** $P_{\max}$ (ordinate) vs. γ' (abscissa). Solid lines represent non-Hermitian charger in Eq. (10) ($\gamma = \gamma'$) while dashed lines represent the Hermitian ones ($\gamma = -i\gamma'$), representing the XY model. The ground state of non-interacting Battery Hamiltonian represents the initial state of the QB as in Fig. 9. Different choices of $h_{i(r)}$ in non-Hermitian and Hermitian cases are mentioned in legends. The system size is taken to be six, i.e., $N = 6$. Both the axis are dimensionless.

ones $\forall\, \gamma'$. For high γ', eg. for $\gamma' \geq 0.6$, the maximum generated power, P_{max}, is small for Hermitian case and in this regime, non-Hermitian advantage is more pronounced than that of low γ'.

2. Let us consider the case with $h_{i(r)} \sim 1.005$. In this domain, both non-Hermitian and Hermitian charging lead to a almost same P_{max} value, thereby exhibiting no adavantage. Interestingly, $\delta^{\mathcal{RT}}_{P_{\max}}$ vanishes with the increase of N.

3. Going beyond $h_{i(r)} > 1$, eg., 1.5, the performance of the QB in terms of $P_{\max}$ with Hermitian charger outperforms the corresponding non-Hermitian QB.

Therefore, the close inspection reveals that like the $\mathcal{PT}$-symmetric charger, the $\mathcal{RT}$-symmetric charging Hamiltonian has potential to give benefit provided the charging Hamiltonian is tuned in a suitable way.

Effect of system size on P_{max}. It is natural to ask whether the improvements remain valid even when one wants to design a battery with a reasonable system size. Until now, it is exhibited for $N = 2$ and 6. For a fixed γ', we check whether the advantage is just an numerical artifact or not by comparing P_{max} with N for different exemplary values of $h_{i(r)}$. As depicted in Fig. 11, we observe that $P_{\max}$ saturates to a fixed value irrespective of γ' values and the strength of the magnetic fields, h_i and h_r. Hence $P_{\max}$ of a QB consisting of a reasonable number of lattice sites continues to be advantageous in the non-Hermitian case provided the magnetic field in the charger is adjusted properly.

Temperature dependence of power. We have already observed some non-trivial effects on the power output of the QB

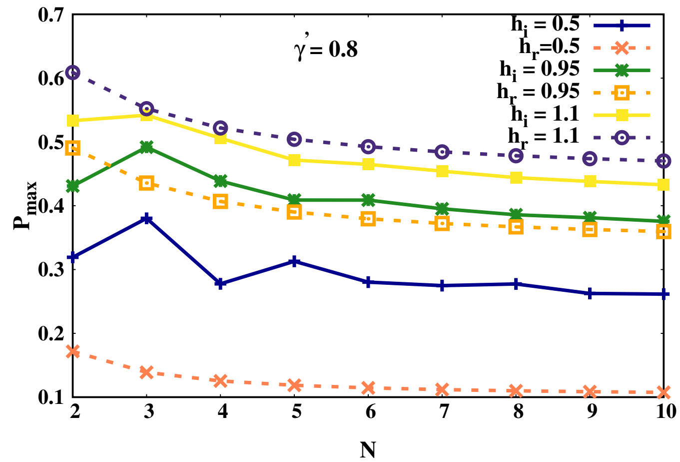

FIG. 11. **Scaling of QB with $\mathcal{RT}$-symmetric charger.** $P_{\max}$ (y-axis) vs. N (x-axis) for $\gamma' = 0.8$. Different choices of $h_{i(r)}$ in non-Hermitian (solid) and Hermitian (dashed) cases are mentioned in legends. All other specifications are same as in Fig. 10. Both the axes are dimensionless.

with $\mathcal{PT}$-symmetric charger when the initial state is the thermal state, ρ_β with $\beta = \beta'/|J|$. It increases with the decrease of temperature (see Fig. 12), thereby showing detrimental effects on power in presence of thermal fluctuation. Like the $\mathcal{PT}$-symmetric case, $P_{\max}$ is close to zero in the limiting case, i.e., $\beta \to 0$ although it does not vanish exactly like the unitary dynamics. Interestingly, however, that $\delta^{\mathcal{RT}}_{P_{\max}}$ is small when the temperature is moderately high. In other words, the superiority of non-Hermitian (Hermitian) systems over Hermitian (non-Hermitian) ones gets pronounced with a moderate temperature of the initial state of the QB.

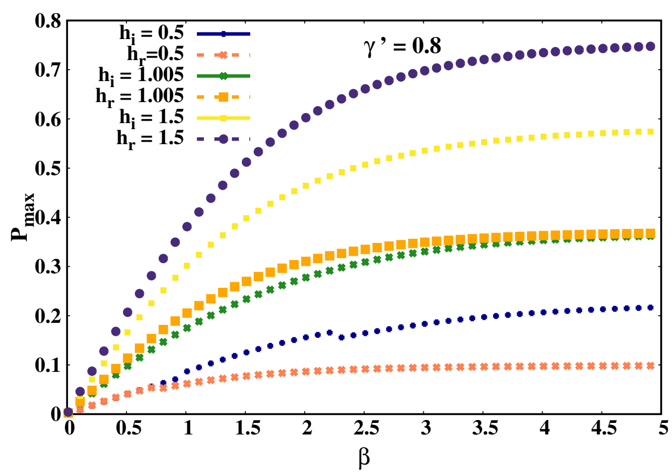

FIG. 12. **Effects of thermal fluctuations on non-Hermitian battery.** The maximal power (ordinate) against $\beta = \beta'/|J|$ (abscissa) where the initial state is prepared as the thermal state of the battery. The charging is again by the $\mathcal{RT}$-symmetric Hamiltonian with $\gamma' = 0.8$. All other specifications are same as in Fig. 10. Both the axes are dimensionless.

V. CONCLUSION

The dynamics of quantum systems governed by the non-Hermitian Hamiltonian have attracted lots of attention in recent times. On the other hand, the evolution of a quantum system plays an important role to build quantum technologies, like thermal machines. Among several quantum thermal devices, a prominent one is the quantum battery which shows a better storage capacity with the help of quantum mechanics than the classical models.

We incorporated non-Hermitian evolution in constructing quantum batteries (QB). Specifically, we use both $\mathcal{PT}$- and $\mathcal{RT}$-symmetric charging Hamiltonian to charge the ground state of an interacting and non-interacting Hamiltonians respectively. When the battery consists of two sites, we analytically proved that the maximum power with non-Hermitian chargers gets enhanced compared to their Hermitian counterparts provided the system parameters are tuned appropriately. In the case of local $\mathcal{PT}$-symmetric charger, when the initial state of the QB is the ground state of XY model with the transverse magnetic field having a moderate system size, we demonstrate that it can produce extractable power which cannot be obtained with the QB Hamiltonian without interactions, thereby showing quantum advantage. Moreover, we find that the power scales with $\sqrt{\text{system size}}$, thereby exhibiting the persistence of non-Hermitian advantage even in the macroscopic limit.

Starting with the ground state of the non-interacting Hamiltonian, we demonstrated that the interacting $\mathcal{RT}$-symmetric charger have also potential to generate a higher amount of power in the QB than that of the corresponding Hermitian charger provided the magnetic field in the charging is adjusted appropriately. We also observed that the power also saturates to a nonvanishing finite value both in the Hermitian and non-Hermitian scenarios with the increase of system size.

Beyond the zero-temperature scenario, if the initial state of the battery is the thermal state and the charging Hamiltonian is non-Hermitian, the interesting non-trivial results emerge – as expected, the maximum power decreases with the increase of temperature although unlike Hermitian systems, it does not vanish at infinite temperature.

The construction of quantum battery proposed in the framework of non-Hermitian quantum mechanics and the advantages reported here opens up a possibility to design other quantum technologies including quantum heat engines, refrigerators in this paradigm. It will be an interesting direction to explore the possible implementations of these devices using currently available technologies.

ACKNOWLEDGMENTS

We acknowledge the support from the Interdisciplinary Cyber Physical Systems (ICPS) program of the Department of Science and Technology (DST), India, Grant No.: DST/ICPS/QuST/Theme- 1/2019/23, the use of QIClib – a modern C++ library for general purpose quantum information processing and quantum computing (https://titaschanda.github.io/QIClib), and the cluster computing facility at the Harish-Chandra Research Institute.

VI. APPENDIX

Battery based on $\mathcal{PT}$-symmetric charger. The evolved state of a system consisting of two lattice sites at later time t with the evolution operator constructed via $H^{\mathcal{PT}}_{charging}$ reads as

$$|\psi(t)\rangle = \begin{pmatrix} -\frac{\cos^2\alpha\csc^2(t\cos\alpha)}{\cos^4(\alpha+t\cos\alpha)\csc^4(t\cos\alpha)+\cos^2(\alpha+t\cos\alpha)\csc^2(t\cos\alpha)+1} \\ -\frac{i\cos^2(\alpha)\cos(\alpha+t\cos(\alpha))\sin(t\cos(\alpha))}{\cos^4(\alpha+t\cos(\alpha))+2\sin^2(t\cos(\alpha))\cos^2(\alpha+t\cos(\alpha))+\sin^4(t\cos(\alpha))} \\ -\frac{i\cos^2(\alpha)\cos(\alpha+t\cos(\alpha))\sin(t\cos(\alpha))}{\cos^4(\alpha+t\cos(\alpha))+2\sin^2(t\cos(\alpha))\cos^2(\alpha+t\cos(\alpha))+\sin^4(t\cos(\alpha))} \\ \frac{\cos^2(\alpha)}{\sec^2(\alpha+t\cos(\alpha))\sin^4(t\cos(\alpha))+\sin^2(t\cos(\alpha))+\cos^2(\alpha+t\cos(\alpha))}, \end{pmatrix} \tag{12}$$

where the initial state $|\psi(0)\rangle = |0001\rangle$ is the ground state of the Hamiltonian, H_B when $J \in [-2h, 2h-0.1]$. We can express the form of the power which depends on the parameter of the system, given by

$$P^{\mathcal{PT}}(t,h,J,\alpha) = \frac{-h\cos^4(\alpha+t\cos(\alpha)) + h\sin^4(t\cos(\alpha)) + J\cos^2(\alpha+t\cos(\alpha))\sin^2(t\cos(\alpha))}{ht\left(\cos^4(\alpha+t\cos(\alpha)) + 2\cos^2(\alpha+t\cos(\alpha))\sin^2(t\cos(\alpha)) + \sin^4(t\cos(\alpha))\right)} + \frac{1}{t}. \tag{13}$$

We now, calculate the power generated when the $H^{\mathcal{PT}}_{charging}$ is replaced with its Hermitian counterpart as

$$H^{herm}_{charging} = \sum_{r=1}^{N} [\sigma^x_r + \sin(\alpha)\sigma^z_r]\,. \tag{14}$$

In the Hermitian domain, the instantaneous power takes the form as

$$P^{herm}(t,h,J,\alpha) = \frac{-h\cos(4\alpha) + \cos(2\alpha)(8h-2J) + \cos\left(t\sqrt{6-2\cos(2\alpha)}\right)(\cos(2\alpha)(4h+2J) - 12h - 2J) - 7h - J\cos\left(2t\sqrt{6-2\cos(2\alpha)}\right) + 3J}{ht(-6\cos(2\alpha) + 0.5\cos(4\alpha) + 9.5)} + \frac{1}{t}. \tag{15}$$

Comparing $P^{\mathcal{PT}}(t,h,J,\alpha)$ and $P^{herm}(t,h,J,\alpha)$, and optimizing over time, we can find that the difference is positive in $J \in [-2h, 2h-0.1]$, thereby establishing non-Hermitian enhancement.

QB with $\mathcal{RT}$-symmetric charger. The ground state of the normalized Hamiltonian, H_B^{n-int} which is the initial state of the QB reads as

$$|\psi(0)\rangle = \frac{1}{2}\begin{pmatrix}1\\-1\\-1\\1\end{pmatrix},$$

with eigenvalue $=-1$. The evolution operator based on $H^{\mathcal{RT}}_{charging}$ acts on the initial state and produces the evolved state, given by

$$|\psi(t)\rangle = \frac{1}{\text{tr}(e^{-iH^{\mathcal{RT}}_{charging}t}|\psi(0)\rangle)}e^{-iH^{\mathcal{RT}}_{charging}t}|\psi(0)\rangle,$$

which reduces to

$$|\psi(t)\rangle = \frac{1}{\sqrt{\mathcal{N}}}\begin{pmatrix}A\\B\\B\\C\end{pmatrix}.$$

Here

$$A = \frac{\gamma\sinh\left(\frac{1}{2}t\sqrt{\gamma^2-4h^2}\right)}{2\sqrt{\gamma^2-4h^2}} + \frac{1}{2}\left(\cosh\left(\frac{1}{2}t\sqrt{\gamma^2-4h^2}\right) - \frac{2ih\sinh\left(\frac{1}{2}t\sqrt{\gamma^2-4h^2}\right)}{\sqrt{\gamma^2-4h^2}}\right),$$
$$B = -\frac{\cos(t/2)}{2} + \frac{i\sin(t/2)}{2},$$
$$C = \frac{\gamma\sinh\left(\frac{1}{2}t\sqrt{\gamma^2-4h^2}\right)}{2\sqrt{\gamma^2-4h^2}} + \frac{1}{2}\left(\cosh\left(\frac{1}{2}t\sqrt{\gamma^2-4h^2}\right) + \frac{2ih\sinh\left(\frac{1}{2}t\sqrt{\gamma^2-4h^2}\right)}{\sqrt{\gamma^2-4h^2}}\right),$$
$$\text{and } \mathcal{N} = \frac{\gamma\sqrt{\gamma^2-4h^2}\sinh\left(t\sqrt{\gamma^2-4h^2}\right) + \gamma^2\cosh\left(t\sqrt{\gamma^2-4h^2}\right) + \gamma^2 - 8h^2}{2\gamma^2-8h^2}.$$

We now calculate the power in Eq. (1) when charging is performed by $H^{\mathcal{RT}}_{charging}$ with $\gamma=\gamma'$, given by

$$P^{\mathcal{RT}}(t) = \frac{2\cos\left(\frac{t}{2}\right)\left(\left({\gamma'}^2-4h^2\right)\cos\left(\frac{t}{2}\sqrt{4h^2-{\gamma'}^2}\right) - \gamma'\sqrt{4h^2-{\gamma'}^2}\sin\left(\frac{t}{2}\sqrt{4h^2-{\gamma'}^2}\right)\right)}{t\left|\cos\left(\sqrt{4h^2-{\gamma'}^2}t\right){\gamma'}^2 + {\gamma'}^2 - \sqrt{4h^2-{\gamma'}^2}\sin\left(\sqrt{4h^2-{\gamma'}^2}t\right)g - 8h^2\right|} + \frac{1}{t}, \text{ when } {\gamma'}^2 < 4h^2, \tag{16}$$

and

$$P^{\mathcal{RT}}(t) = 1 - \frac{2\cos\left(\frac{t}{2}\right)\left(\gamma'\sqrt{{\gamma'}^2-4h^2}\sinh\left(\frac{1}{2}t\sqrt{{\gamma'}^2-4h^2}\right) + \left({\gamma'}^2-4h^2\right)\cosh\left(\frac{1}{2}t\sqrt{{\gamma'}^2-4h^2}\right)\right)}{t\left|\cosh\left(\sqrt{{\gamma'}^2-4h^2}t\right){\gamma'}^2 + {\gamma'}^2 + \sqrt{{\gamma'}^2-4h^2}\sinh\left(\sqrt{{\gamma'}^2-4h^2}t\right)\gamma' - 8h^2\right|}, \text{ when } {\gamma'}^2 > 4h^2. \tag{17}$$

When the charger is Hermitian, $H^{herm}_{charging}$ with $\gamma=-i\gamma'$, the generated power can be computed as

$$P_{herm}(t) = 1 - \frac{\frac{\gamma'\sin\left(\frac{t}{2}\right)\sin\left(\frac{1}{2}t\sqrt{{\gamma'}^2+4h^2}\right)}{\sqrt{{\gamma'}^2+4h^2}} + \cos\left(\frac{t}{2}\right)\cos\left(\frac{1}{2}t\sqrt{{\gamma'}^2+4h^2}\right)}{t}, \text{ when } {\gamma'}^2+4h^2 \neq 0. \tag{18}$$

It can be shown that $\delta^{\mathcal{PT}(\mathcal{RT})}_{P_{\max}}$ given in Eqs. (7) and (11) are positive in some parameter regimes, thereby exhibiting the response of non-Hermitian chargers on QB.

[1] N. Gisin, G. Ribordy, W. Tittel, and H. Zbinden, Rev. Mod. Phys. **74**, 145 (2002).

[2] C. H. Bennett, G. Brassard, C. Crépeau, R. Jozsa, A. Peres, and

W. K. Wootters, Phys. Rev. Lett. **70**, 1895 (1993).

[3] C. H. Bennett and S. J. Wiesner, Phys. Rev. Lett. **69**, 2881 (1992).

[4] M. A. Nielsen and I. L. Chuang, *Quantum Computation and Quantum Information* (Cambridge University Press, 2009).

[5] V. Giovannetti, S. Lloyd, and L. Maccone, Nature Photonics **5**, 222 (2011).

[6] C. L. Degen, F. Reinhard, and P. Cappellaro, Rev. Mod. Phys. **89**, 035002 (2017).

[7] N. Linden, S. Popescu, and P. Skrzypczyk, Phys. Rev. Lett. **105**, 130401 (2010).

[8] A. Hewgill, J. O. González, J. P. Palao, D. Alonso, A. Ferraro, and G. De Chiara, Phys. Rev. E **101**, 012109 (2020).

[9] R. Alicki and M. Fannes, Phys. Rev. E **87**, 042123 (2013).

[10] F. Campaioli, F. A. Pollock, and S. Vinjanampathy, arXiv:1805.05507 (2018).

[11] K. Joulain, J. Drevillon, Y. Ezzahri, and J. Ordonez-Miranda, Phys. Rev. Lett. **116**, 200601 (2016).

[12] G. Gemmer, M. Michel, and G. Mahler, *Quantum Thermodynamics* (Springer, New York, 2004).

[13] F. Binder, L. A. Correa, C. Gogolin, J. Anders, and G. Adesso, *Thermodynamics in the Quantum Regime* (Springer, Cham, 2018).

[14] S. Vinjanampathy and J. Anders, Contemporary Physics **57**, 545 (2016), https://doi.org/10.1080/00107514.2016.1201896.

[15] C. Jarzynski, Phys. Rev. Lett. **78**, 2690 (1997).

[16] T. B. Batalhão, A. M. Souza, L. Mazzola, R. Auccaise, R. S. Sarthour, I. S. Oliveira, J. Goold, G. De Chiara, M. Paternostro, and R. M. Serra, Phys. Rev. Lett. **113**, 140601 (2014).

[17] S. An, J.-N. Zhang, M. Um, D. Lv, Y. Lu, J. Zhang, Z.-Q. Yin, H. T. Quan, and K. Kim, Nature Physics **11**, 193 (2015).

[18] D. Ferraro, M. Campisi, G. M. Andolina, V. Pellegrini, and M. Polini, Phys. Rev. Lett. **120**, 117702 (2018).

[19] J. Q. Quach, K. E. McGhee, L. Ganzer, D. M. Rouse, B. W. Lovett, E. M. Gauger, J. Keeling, G. Cerullo, D. G. Lidzey, and T. Virgili, Science Advances **8**, eabk3160 (2022), https://www.science.org/doi/pdf/10.1126/sciadv.abk3160.

[20] X. Nie, X. Zhu, C. Xi, X. Long, Z. Lin, Y. Tian, C. Qiu, X. Yang, Y. Dong, J. Li, T. Xin, and D. Lu, arXiv:2011.12580 (2020).

[21] F. Campaioli, F. A. Pollock, F. C. Binder, L. Céleri, J. Goold, S. Vinjanampathy, and K. Modi, Phys. Rev. Lett. **118**, 150601 (2017).

[22] G. M. Andolina, M. Keck, A. Mari, V. Giovannetti, and M. Polini, Phys. Rev. B **99**, 205437 (2019).

[23] T. P. Le, J. Levinsen, K. Modi, M. M. Parish, and F. A. Pollock, Phys. Rev. A **97**, 022106 (2018).

[24] S. Ghosh, T. Chanda, and A. Sen(De), Phys. Rev. A **101**, 032115 (2020).

[25] D. Farina, G. M. Andolina, A. Mari, M. Polini, and V. Giovannetti, Phys. Rev. B **99**, 035421 (2019).

[26] S. Ghosh, T. Chanda, S. Mal, and A. Sen(De), Phys. Rev. A **104**, 032207 (2021).

[27] S. Ghosh and A. Sen(De), Phys. Rev. A **105**, 022628 (2022).

[28] C. M. Bender and S. Boettcher, Phys. Rev. Lett. **80**, 5243 (1998).

[29] C. M. Bender, Reports on Progress in Physics **70**, 947 (2007).

[30] X. Z. Zhang and Z. Song, Phys. Rev. A **87**, 012114 (2013).

[31] Y.-C. Lee, M.-H. Hsieh, S. T. Flammia, and R.-K. Lee, Phys. Rev. Lett. **112**, 130404 (2014).

[32] J.-S. Tang, Y.-T. Wang, S. Yu, D.-Y. He, J.-S. Xu, B.-H. Liu, G. Chen, Y.-N. Sun, K. Sun, Y.-J. Han, C.-F. Li, and G.-C. Guo, Nature Photonics **10**, 642 (2016).

[33] O. Bendix, R. Fleischmann, T. Kottos, and B. Shapiro, Phys. Rev. Lett. **103**, 030402 (2009).

[34] G. L. Giorgi, Phys. Rev. B **82**, 052404 (2010).

[35] L. G. C. Lakkaraju and A. Sen(De), Phys. Rev. A **104**, 052222 (2021).

[36] A. Guo, G. J. Salamo, D. Duchesne, R. Morandotti, M. Volatier-Ravat, V. Aimez, G. A. Siviloglou, and D. N. Christodoulides, Phys. Rev. Lett. **103**, 093902 (2009).

[37] M. Wimmer, A. Regensburger, M.-A. Miri, C. Bersch, D. N. Christodoulides, and U. Peschel, Nature Communications **6**, 7782 (2015).

[38] J. Schindler, A. Li, M. C. Zheng, F. M. Ellis, and T. Kottos, Phys. Rev. A **84**, 040101 (2011).

[39] M. Kreibich, J. Main, H. Cartarius, and G. Wunner, Phys. Rev. A **90**, 033630 (2014).

[40] L. Jin and Z. Song, Phys. Rev. A **84**, 042116 (2011).

[41] Y. N. Joglekar, D. Scott, M. Babbey, and A. Saxena, Phys. Rev. A **82**, 030103 (2010).

[42] L. Jin and Z. Song, Phys. Rev. A **81**, 032109 (2010).

[43] L. Jin and Z. Song, Phys. Rev. A **80**, 052107 (2009).

[44] S. Yu, Y. Meng, J.-S. Tang, X.-Y. Xu, Y.-T. Wang, P. Yin, Z.-J. Ke, W. Liu, Z.-P. Li, Y.-Z. Yang, G. Chen, Y.-J. Han, C.-F. Li, and G.-C. Guo, Phys. Rev. Lett. **125**, 240506 (2020).

[45] Y. Cao and P. Yan, Phys. Rev. B **99**, 214415 (2019).

[46] J. C. Budich and E. J. Bergholtz, Phys. Rev. Lett. **125**, 180403 (2020).

[47] F. Koch and J. C. Budich, Phys. Rev. Research **4**, 013113 (2022).

[48] Y. Chu, Y. Liu, H. Liu, and J. Cai, Phys. Rev. Lett. **124**, 020501 (2020).

[49] A. McDonald and A. A. Clerk, Nature Communications **11**, 5382 (2020).

[50] J. Q. Quach and W. J. Munro, Phys. Rev. Applied **14**, 024092 (2020).

[51] O. Mandel, M. Greiner, A. Widera, T. Rom, T. W. Hänsch, and I. Bloch, Nature **425**, 937 (2003).

[52] R. Blatt and C. F. Roos, Nature Physics **8**, 277 (2012).

[53] M. Lewenstein, A. Sanpera, V. Ahufinger, B. Damski, A. Sen(De), and U. Sen, Advances in Physics **56**, 243 (2007), https://doi.org/10.1080/00018730701223200.

[54] K. R. K. Rao, H. Katiyar, T. S. Mahesh, A. Sen (De), U. Sen, and A. Kumar, Phys. Rev. A **88**, 022312 (2013).

[55] J. Li, A. K. Harter, J. Liu, L. de Melo, Y. N. Joglekar, and L. Luo, Nature Communications **10**, 855 (2019).

[56] U. Günther and B. F. Samsonov, Phys. Rev. Lett. **101**, 230404 (2008).

[57] K. Kawabata, Y. Ashida, and M. Ueda, Phys. Rev. Lett. **119**, 190401 (2017).

[58] M. Huang, R.-K. Lee, L. Zhang, S.-M. Fei, and J. Wu, Phys. Rev. Lett. **123**, 080404 (2019).

[59] J. Kim, D. Rosa, and D. Šafránek, arXiv preprint arXiv:2108.02491 (2021).